論 文

Transactions of the Society of Naval Architects of Korea
Vol. 32, No. 4, November 1995
大 韓 造 船 學 會 論 文 集
第 32 卷 第 4 號 1995年 11月

Analysis of End-Plated Propellers by Panel Method

by

C.-S. Lee*, I.-S. Moon* and Y.-G. Kim**

패널법에 의한 날개끝판부착 프로펠러의 해석

이창섭*, 문일성*, 김영기**

Abstract

This paper describes the procedure to analyze the performance of the end-plated propeller (EPP) by a boundary integral method. The screw blade (SB) and end-plate (EP) are represented by a set of quadrilateral panels, where the source and normal dipole of uniform strength are distributed.

The perturbation velocity potential, being the only unknown via the potential-based formulation, is determined by satisfying the flow tangency condition on the blade and the end-plate at the same time. The Kutta condition is satisfied through an iterative process by requiring the null pressure jump across the upper and lower sides of the trailing edges of both the SB and the EP.

Sample calculations indicate that the EP increases the loading near the tip of the SB while spreading the trailing vortices along the trailing edge of the EP, thus avoiding the strong tip-vortex formation. Predicted performance of the EPP shows good correlations with the experimental results. The method is therefore considered applicable in designing and analyzing the EPP which may be an alternative for energy-saving propulsive devices.

요 약

본 논문은 경계적분법에 의해 날개끝판이 부착된 프로펠러(EPP)의 성능을 해석하는 방법을 기술하고 있다. 나선 프로펠러 날개와 날개끝판을 사각형 판요소로 치환하고, 균일 세기의 쏘오스와

발 표 : 1994년도 12월 8일 제9차 추진기/캐비테이션 분과 워크샵
접수일자 : 1994년 6월 14일, 재접수일자: 1995년 10월 20일
* 정회원, 충남대학교 선박해양공학과
** 정회원, 삼성중공업 (주) 중앙연구소

법선 다이폴을 분포하여 해석한다. 포텐셜을 기저로하는 정식화 과정을 통해 적분방정식을 구하고, 나선날개와 날개끝판에서 동시에 법선방향 비침투조건을 만족시킴으로써 섭동 속도 포텐셜을 구하였다. Kutta조건은 반복작업을 통해 나선날개와 날개끝판의 뒷날에서 압력점프가 없어지도록 함으로써 만족시켰다.

예제계산을 통하여 날개끝판이 나선날개의 날개끝 부근의 하중을 증가시킴을 보였고, 동시에 날개끝판의 뒷날에 걸쳐 후연 보오텍스를 분산시킴으로써 강력한 날개끝 보오텍스의 형성을 피할 수 있음을 확인하였다. EPP의 성능을 추정한 결과는 실험결과와 좋은 일치를 보인다. 에너지절약 추진장치로 채택될 수 있는 EPP의 설계 및 해석을 위하여 본 연구에서 확립된 방법이 적용가능하리라 판단된다.

1. Introduction

The propulsive device with an improved efficiency is ever in need regardless of the oil prices in the world oil markets. The efficiency of the conventional propeller (CVP) reaches almost its maximum point for a given blade outline and a section thickness form.

Our desire to extend the upper limit of the CVP can only be satisfied by introducing another device in the neighborhood of the CVP. Some of the effective devices are based on the design concept that the rotational kinetic energy be minimized by forcing the circumferential velocities induced by each part of the compound propulsor components to cancel each other. The contra-rotating propellers and the pre- and post-swirl vanes are good examples of such designs.

The shape factors of the blade other than the pitch and camber are less influential in the propulsive performance. When the propeller is lightly loaded and operates in uniform inflow, we know that the optimum circulation in the radial direction is elliptical. We do not know yet whether we can improve the efficiency further by increasing the loading near the tip region. Efforts in this direction so far are not promising, since the heavy load at the tip causes the tip vortex separation and the severe cavitation in these region. We may however attach an EP to suppress such undesirable phenomena, while keeping the favorable lift-increasing effect of the EP.

The effect of the EP attached to the propeller blade tip is not thoroughly studied and hence not yet fully understood. When applied to the wing, the end-plate is known to increase the circulation near the tip as well as the lift-drag ratio (see for example Hess[1]). The end-plate attached to the conventional rudder is also known to increase the performance of the rudder. Early application of the EP by Goodman[2] to the model propeller was however unsuccessful due to the heavy cavitation at the EP itself and also due to the increase of the viscous drag of the EP. The experiments of Ito et al[3] and Ito[4] reveals however that 1-4 percent efficiency increase is achievable. They attached two different winglets on the suction and pressure sides of the blade. More extensive studies on the EPP have been carried out in Netherlands, spanning from the early theoretical study by Sparenberg[5] to the recent works of van Gent et al[6] and de Jong et al[7]. By applying the optimizing technique, de Jong[8] obtained the geometry of an optimum EP for a given propeller. They claimed that the efficiency gain could reach 2 - 3 percent above the propeller without EP.

A method to analyze the performance of the EPP is not yet well established. The vortex lattice method(DVM), for example that of Kerwin and Lee[9], successfully applied for the analysis of the CVP, is not suitable in describing the flow behavior at/near the junction of the SB and the EP due to the difficulties in evaluating the correct velocity

near the concentrated discrete vortex filament. The surface panel method, especially based on the potential formulation, is therefore expected to be suitable for the EPP analysis, since the induced otential at a field point very close to and right angle to the panel element can be evaluated much more accurately than in the DVM.

In this paper, we describe briefly the potential-based formulation, which may be found in many other literature(see for example, Morino[10], Lee[11], Hoshino[12] or Kim et al[13]). The performance of the CVP is now accurately predicted by surface panel method, and is well established. We will not go through the detail, especially the description regarding the geometry and the numerical problem associated with the conventional screw propeller. See Kim et al[13] for the details which are not treated in the present paper. The major achievement of the present work is to incorporate a hydrofoil of complex geometry to the blade tip. The application of the dynamic form of the Kutta condition is the most troublesome part of the coding. Due to extension of the EP from the blade to two different sides, the numerical form of the Kutta condition should be carefully applied, which will be described in detail later. Predicted performance of a sample EPP shows a good correlation with the experimental results of de Jong et al[7]. The influence of the EP with varying geometry is examined.

2. Statement of boundary-Value problem

Let us consider an EPP operating in a uniform inflow field. The fluid is assumed to be inviscid, irrotational and incompressible. Conservation of mass to the fluid volume V enclosed by the SB and EP surfaces and their trailing vortex sheets leads to the governing equation for the perturbation velocity potential ϕ as:

$$\nabla^2\phi(p)=0,\ p(\vec{x})\in V \tag{1}$$

where $p(\vec{x})$ denotes a field point in V.

Motion of the fluid satisfying the Laplace equation(1) can be uniquely defined by imposing the appropriate boundary conditions on the boundary surfaces as follows:

1. Quiescence condition at infinity S_∞:

$$\nabla\phi\to 0,\ p(\vec{x})\in S_\infty \tag{2}$$

2. Kinematic boundary condition on the SB and EP surfaces $S_{B\cup E}$:

$$\hat{n}\cdot\vec{U}_\infty+\frac{\partial\phi}{\partial n}=0,\ p(\vec{x})\in S_{B\cup E} \tag{3}$$

where $\vec{U}_\infty$ is the oncoming velocity to the propeller.

3. Kutta condition at the trailing edge of the SB and the EP:

$$|(\nabla\phi)_{T.E.}|<\infty \tag{4}$$

4. Kinematic and dynamic boundary conditions on the wake surface S_W:

$$\Delta\frac{\partial\phi}{\partial n}=(\hat{n}\cdot\nabla\phi)^+-(\hat{n}\cdot\nabla\phi)^-=0 \tag{5}$$

$$\Delta p=p^+-p^-=0 \tag{6}$$

where p denotes the pressure, and + and - denote the upper and lower surface of the wake, respectively.

5. Conservation of circulation:

$$\frac{D\Gamma}{Dt}=0 \tag{7}$$

3. Integral Equations

From the Green's theorem, we may first derive an expression for the perturbation potential in the flow field by distributing the normal dipoles and sources on the solid surfaces, and the normal dipoles on the shed vortex sheet.

The perturbation velocity potential in the fluid region may now be expressed as follows:

$$\phi(\vec{x}) = \int_{S_B \cup E} \{-\phi(\vec{\xi})\} \frac{\partial}{\partial n_\xi} G(\vec{x};\vec{\xi})\, dS + \int_{S_B \cup E} \left\{\frac{\partial \phi}{\partial n}(\vec{\xi})\right\} G(\vec{x};\vec{\xi})\, dS + \int_{S_w} \{-\Delta\phi\}_w \frac{\partial}{\partial n_\xi} G(\vec{x};\vec{\xi})\, dS \quad (8)$$

where $G(\vec{x};\vec{\xi})$ is the Green's function.

Due to the characteristics of singularities, the governing equation(1), and the quiescence condition (2), will automatically be satisfied.

We know the strength of the sources distributed on the SB and EP surfaces from (3) and the strengths of the shed dipoles on the trailing vortex sheets in terms of the dipoles on the SB or the EP by satisfying Kelvin's conservation of circulation. We now note that (8) becomes an integral equation for the unknown strengths of normal dipoles on the SB and EP surfaces. Here the potential function is the only unknown in the integral equation.

4. Discretization of Solid Surfaces

4.1 Screw blade surface

For numerical computation, the screw blade and end-plate surfaces are subdivided into a set of quadrilateral panel elements. As shown in Fig. 1, the blade is discretized into M_p strips from the hub radius r_H to the tip radius R in the spanwise direction, and N_p panels around the chordwise section.

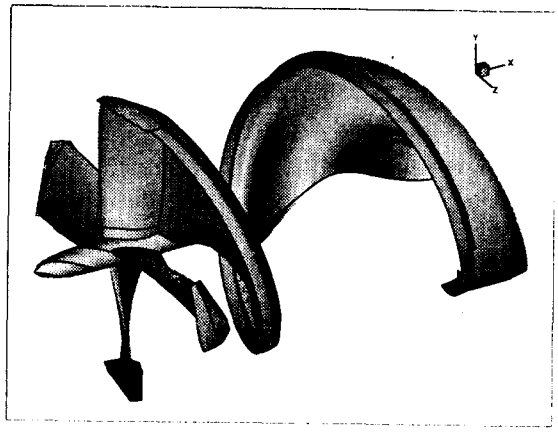

Fig. 1 Perspective view of EPP with trailing vortex sheet.

Table 1 Principal characteristics for end-plate a propeller with 4 blade

r/R	P/D	Rake /D	Skew (deg.)	Chord /D	f/c	t/c
0.183	285.5	0.	0.	43.649	1.871	9.919
0.238	294.9	0.	0.	44.674	2.137	9.536
0.293	294.3	0.	0.	46.147	2.369	8.981
0.405	284.7	0.	0.	50.008	2.835	7.713
0.517	277.4	0.	0.	53.608	2.896	6.463
0.629	271.7	0.	0.	57.103	2.688	5.287
0.741	267.5	0.	0.	60.034	2.316	3.988
0.853	263.7	0.	0.	62.392	1.962	2.905
0.908	262.0	0.	0.	63.211	1.860	2.457
0.964	261.1	0.	0.	63.683	1.859	2.283
1.000	260.3	0.	0.	63.834	1.872	2.227

As in Kim et al[13], a half-cosine discretization spacing is adopted here in the spanwise direction and the cosine spacing in the chordwise directions with $M_p = 10$ and $N_p = 40$.

4.2 End-plate surface

The end-plate is a hydrofoil attached perpendicular to the tip of the screw blade.

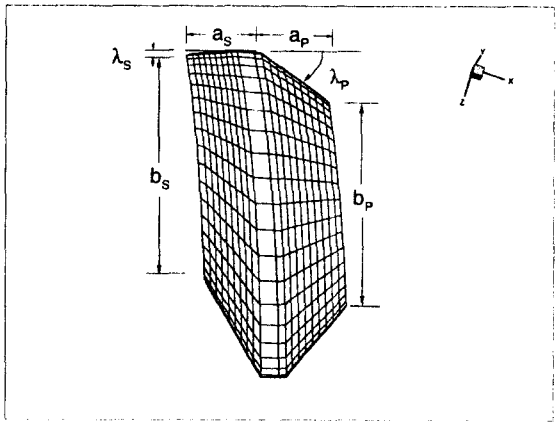

Fig. 2 Definition of parameters for end-plate geometry.

The end-plates for the suction and pressure sides of the SB are designed separately, designated respectively as SEP and PEP. To define the EP surfaces, we introduce a set of geometric parameters as shown in Fig. 2, where λ denotes the sweptback angle, and a and b the span and the tip chordlength, respectively. The subscripts s and p denote the suction and pressure sides of the SB, respectively. In the present study, we adopted an NACA 66 thickness form to build the EP, while the maximum thickness tapers to zero elliptically towards the end-plate tip. We did not consider the effect of the camber of the EP in the present analysis to reduce the work scope.

5. Modeling of Trailing Wake

Due to the action of the propeller, the axial velocity within the slipstream tube is increased and the radius of the tube is contracted. The exact location of the trailing vortex sheet should in principle be determined by satisfying the kinematic and dynamic boundary conditions on the wake surface as a part of the solution. Instead of solving the exact trailing vortex geometry, we adopt without proof the model of Greeley and Kerwin[14] developed for the CVP.

The true shape of the wake trailing the EP is not known either and there is little experimental data available. We therefore assume that the wake follows the lines similar to the tip vortex trajectory obtained at the tip panel of the SB.

Fig. 1 also shows the shed vortex wake trailing both the SB and the EP. The validity of this approximation should however be verified by a direct measurement of the slipstream region, since the geometry of the wake trailing the SB and the EP give influence on the performance of EPP most significantly.

6. Numerical Procedure

6.1 Calculation of induced potential

The potential ϕ and the normal derivative $\partial\phi/\partial n$ are assumed constant on each panel, and hence the potential at a field point $\vec{x}$ may be expressed as follows:

$$\begin{aligned}\phi(\vec{x}) &= \sum_j \{-\phi\}_j \int_{S_j} \frac{\partial}{\partial n_\xi} G(\vec{x};\vec{\xi})\,dS \\ &+ \sum_j \left\{\frac{\partial\phi}{\partial n}\right\}_j \int_{S_j} G(\vec{x};\vec{\xi})\,dS \\ &+ \sum_{ju} \{-\Delta\phi\}_{ju} \int_{S_{ju}} \frac{\partial}{\partial n_\xi} G(\vec{x};\vec{\xi})\,dS\end{aligned} \tag{9}$$

where the subscript j spans over the SB and the EP, and ju over the trailing wake.

Induced potentials due to the normal dipoles and sources distributed on the hyperboloidal surface panel may be computed by formulae suggested by Morino[10].

6.2 Kutta condition

The numerical Kutta condition we adopted in the present paper is the same as that suggested by Suh et al[15]. Through an

iterative process the pressure jump at the trailing edge of both the SB and the EP is forced to vanish.

If the end-plate is present only on one side of the screw blade, the end-plate is considered a part of the extended screw blade, and hence no special difficulty in coding is expected. Since the end-plates are attached on both sides of the blade in the present study, special care is necessary to correctly deal with the dynamic form of numerical Kutta condition. We require that the potential be continuous on the same side of the SB and the EP inner surface, while the potential be continuous all along the trailing edge on the outer surface of the EP. In fact the nonzero circulation at the screw blade tip are divided into three parts; one component into the SEP, the other into the PEP and the third shedding into the trailing wake at the tip. The role of the EP is to spread the vorticity more uniformly from the trailing edge into the trailing wake downstream, thus avoiding the formation of the strong tip vortex and hence delaying the inception of the tip vortex cavitation.

6.3 Solution procedure

The boundary conditions on the SB and EP surfaces are satisfied on the geometric center of each quadrilateral panel. By applying the discretized expression (9) for the potential to the control points over the SB and EP surfaces, we obtain a set of linear simultaneous equations for the unknown dipole strengths, which may be easily solved numerically.

Once the strengths of the normal dipoles are obtained, the velocities on the SB and the EP are computed by differentiating the potentials on the surfaces, and subsequently the pressures and forces are obtained.

7. Numerical Analysis and Results

7.1 Test propellers

To validate the present formulation and numerical procedure, we selected a 4-bladed propeller, designed by de Jong et al[7], with a Kaplan type blade outline as shown in Fig. 1 and then attached the EP's to form the SEP and PEP as shown in Fig. 2. The end-plate is made of NACA 66(mod) thickness form, whose thickness is tapered to zero towards the tip elliptically. The geometry of the SB and the EP and the experimental results carried out with and without the EP are available in de Jong et al[7]. The exact shape of the EP of the de Jong et al can not be easily duplicated and hence is replaced by two different hydrofoils generated with $\lambda_s = 10^{\circ}$, $\lambda_p = 40^{\circ}$ and $a_s = a_p = 0.2$, and $b_s = b_p = 0.25$. The thickness at the root of the EP is arbitrarily chosen to be the same as the thickness at the tip of the SB.

7.2 Performance prediction

The open-water characteristics are then computed for three different advance coefficients, $J_A = 0.524$, 0.624 and 0.724, with the skin friction coefficient $C_F = 0.004$ corresponding to the model test $R_n = 2 \times 10^6$.

Fig. 3 shows the predicted thrust and torque coefficients and the efficiency for the EPP together with the corresponding results obtained for the propeller without the EP. The result of the experiments, carried out at MARIN, is reproduced from de Jong et al[7].

It may be first of all observed that, for the propeller without the EP, the thrust coefficient predicted by the panel method of Kim et al[13]

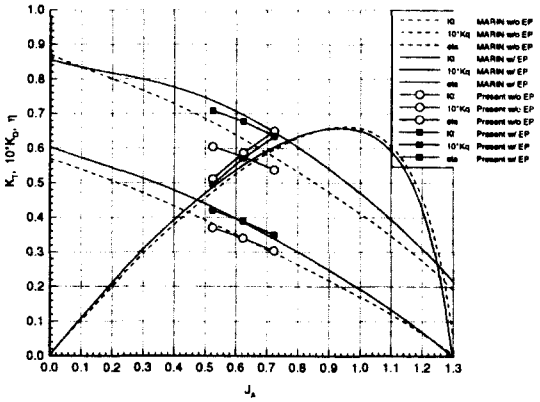

Fig. 3 Open-water characteristics of the EPP: present predictions are compared with experiments of de Jong et al[7].

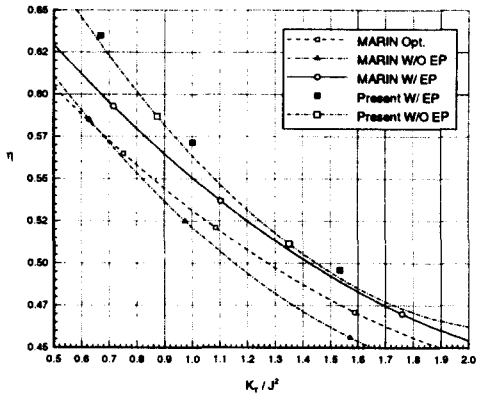

Fig. 4 Comparison of propeller efficiencies on the basis of equal thrust: present predictions are compared with experiments of de Jong et al[7].

correlates well with the de Jong's experimental results, whereas the torque coefficient is underestimated compared to the experiments. This is presumably due to the flow separation near the wide-chorded blade tip of Kaplan-type screw blade.

The correlation between the experiments of de Jong et al and the present prediction for the EPP is surprisingly good, although the exact EP shape is not reproduced, contrary to the ill-correlation of the propeller without the EP. This is because the end-plate plays the role favorably in controlling the flow near the wide-chorded tip region.

Due to the action of the EP, the total thrust of the EPP is larger than that without the EP. To produce the required thrust with the same cavitation margin, it is therefore possible to reduce the expanded area of the propeller, thus decreasing the frictional drag. This effect is not studied here, but should be included when global optimization of the propulsor is carried out. Even with the same blade area, the efficiency of the propellers with different geometries should be compared at the same K_T/J_A^2 values. Fig. 4 is also reproduced from de Jong et al and the present result is added. In the figure the efficiency gain $\Delta\eta/\eta_{ref}$ is about 4%. The reference propeller is the optimum one obtained from the B-Series propeller. It is seen that the increase in loading near the tip of the SB results in efficiency gain over the optimum propeller without the EP.

Fig. 5 shows the circulation distribution on the screw blade of the EPP together with that of the original propeller without the EP and also those on the SEP and the PEP. Note first that the circulation on the screw blade near the tip does not decrease to zero value due to the wall effect of the EP, which is expected to increase the lift-drag ratio in this tip area. The circulation is clearly increased from that without the EP. Note then that the circulations in both tipwise directions on the end-plates have different signs, but the trailing vortices shedding from both EP's have the same sign. Thus the spreading effect of the EP is clearly

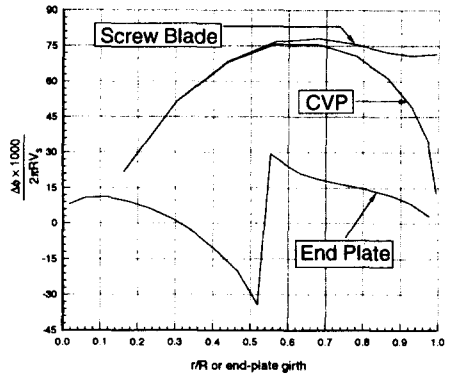

Fig. 5 Circulation distribution on SB and EP.

observed in this figure. The nonzero circulation at the SB tip is divided into two major components, that is, the circulation jump between the SEP and the PEP is observed close to the circulation at the SB tip. This implies that the shed vortex at the SB tip will be very weak and hence it less likely to have a tip vortex cavitation at the SB.

Unlike the case of the aeroplane wing, the effect of the EP on the marine propeller is seriously deteriorated by the viscous drag. It is therefore essential to optimize the EP area by minimizing the viscous torque acting on the EP, while maintaining the favorable wall effect. In the future a series of EPP will be designed by systematically varying the span and the tip chordlength, that is, a and b of the EP and the sweptback angle λ for both EP's.

8. Conclusions

A numerical method to analyze the effect of the end-plate on the conventional screw propeller is now established.

1. A potential-based boundary integral method treating the end-plate geometry is formulated and solved numerically. The method is considered to correctly predict the flow behavior around the junction of the screw blade and the end-plate.
2. The dynamic form of the Kutta condition is applied to the trailing edge of both the screw blade and the end-plate.
3. The role of the end-plate may be summarized as follows:
   - The end-plate increases the loading near the screw blade tip. For the same cavitation margin, the expanded area may be reduced resulting in the increase of the efficiency.
   - For the same K_T/J_A^2, the efficiency of the end-plated propeller is higher than the optimum efficiency of the conventional propeller.
   - Finite nonzero circulation is split and continued into two end-plates having opposite directions, and hence the strength of the tip vortex is roughly reduced by a factor of two, leading ultimately to the increase of the pressure head. Weakened shed vortex is less susceptible to cavitation.
   - End-plates play the role of the flow regulating device, delaying the unfavorable flow phenomena, as evidenced for the Kaplan type blade outline.
4. The present method may be applicable to optimization of the end-plated propellers.

Acknowledgement

The financial support of the Korean Science and Engineering Foundation is greatly acknowledged.

References

[1] Hess, J., "Calculation of potential flow

about arbitrary three-dimensional lifting bodies," Report No. MDC J5679-01, McDonnell Douglas Corp., Oct. 1972, 160p.

[2] Goodman, T. and Breslin, J., "Feasibility study of the effectiveness of tip sails on propeller performance," Stevens Inst. of Tech., MA-RD-940-81006, Sept., 1980

[3] Ito, S., Tagori, T., Ishii, N. and Ide, T., "Study of the propeller with small blades on the blade tips (1st Report)," *J. of SNAJ*, Vol. 159, 1986, pp. 82-90

[4] Ito, S., "Study of the propeller with small blades on the blade tips (2nd Report: Cavitation characteristics)," *J. of SNAJ*, Vol. 161, 1987, pp. 82-91

[5] Sparenberg, J.A. and de Vries, J., "An optimum screw propeller with end plates," Int'l Shipbuilding Progress, Vol. 34, July 1987, pp. 124-133

[6] van Gent, W. and Falcao de Campos, J. and de Jong, K., "Model test results of an optimum propeller with end plates and some practical aspects of application," MARIN Jubilee Meeting, Wageningen, May 1992

[7] de Jong, K., Sparenberg, J., Falcao de Campos, J. and van Gent, "Model testing of an optimally designed propeller with two-sided shifted end plates on the blades," 19th Symp. on Naval Hydrodynamics, Seoul, August 24-28, 1992

[8] de Jong, K., "On the optimization and the design of ship screw propellers with and without end plates," Thesis, Univ. of Groningen, Dept of Mathematics, Nov. 1991

[9] Kerwin, J. E. & Lee, C.-S., "Prediction of steady and unsteady marine propeller performance by numerical lifting surface theory," *Trans. SNAME*, Vol. 86, Soc. of Naval Arch. & Marine Eng., 1978, pp. 218-258

[10] Morino, L. and Kuo, C.-C., " Subsonic potential aerodynamic for complex configurations: a general theory," *AIAA Journal*, Vol. 12, No. 2, 1974, pp. 191-197.

[11] Lee, J.-T., "A potential-based panel method for the analysis of marine propellers in steady flow," Ph.D. Thesis, Department of Ocean Engineering, M.I.T., Cambridge, Mass., 1987.

[12] Hoshino, T., "Hydrodynamic analysis of propellers in steady flow using a surface panel method," *J. of Soc. of Naval Arch. of Japan*, Vol. 165, 1989, pp. 55-70.

[13] Kim, Y.-G., Lee, J.-T., Lee, C.-S. and Suh, J.-C., "Prediction of steady performance of a propeller by using a potential-based panel method," *J. of SNAK*, Vol. 30, No. 1, Feb. 1993, pp. 73-86.

[14] Greeley, D.S. & Kerwin, J.E., "Numerical methods for propeller design and analysis in steady flow," *Trans. SNAME*, Vol. 90, 1982.

[15] Suh, J.-C., Lee, J.-T. and Suh, S.-B., "A bilinear source and doublet distribution over a planar panel and its applications to surface panel method," 19th Symp. on Naval Hydrodynamics, Session XIII, Seoul, August 24-28, 1992, pp. 102-112.